e-ISSN 2580 – 0752

Bulletin of Geology
e-ISSN 2580-0752

Fakultas Ilmu dan Teknologi Kebumian
Institut Teknologi Bandung
www.buletingeologi.com

MULTIPARAMETER LAND SUBSIDENCE VULNERABILITY ASSESSMENT THROUGH SATELLITE IMAGERY, GIS, AND SPATIAL DATA INTEGRATION

S. D. Prayudi[1,*], M. R. Maulana[2], A. Rahmawati[2], D. Arrofi[1], S. Aghnia[3]

1. Department of Geosciences, King Fahd University of Petroleum & Minerals, Dhahran, 31261, Kingdom of Saudi Arabia
2. Department of Geological Engineering, Diponegoro University, Semarang, 50275, Indonesia
3. Department of Geological Engineering, Gadjah Mada University, Yogyakarta, 55281, Indonesia

*Correspondence email: sinatrya.diko@gmail.com

Abstract. Land subsidence is a substantial issue today, particularly in some regions where it has the ability to interrupt future development, halt the process, and even modify the development plan. This study generally focuses on updating current knowledge on land subsidence and performing risk assessments using a case study in Semarang City, Central Java, where land subsidence is a serious problem. Several satellite imageries, such as Sentinel-1 and Sentinel-2, are used as databases in this work, with various target analysis and Geographic Information Systems (GIS) methods used to handle and alter the data. Sentinel-1's radar data, along with the displacement analysis approach of Differential Interferometry Synthetic Aperture Radar (DInSAR), is primarily used to provide a snapshot of the present state of land subsidence under this area in 2022. The result demonstrates the variation of vertical displacement values ranging from -7.7 to 6.65 cm with subsidence spread primarily on the northern region, using two datasets with 60-day intervals between January and March. Using a combination of the Normalize Difference Vegetation Index (NDVI) and the Normalize Difference Built-in Index (NDBI) to create Built-up Index (BU) data, the Sentinel-2 data with optical-based images was then used to map the human-made feature and expansions, notably buildings. Each piece of information considered multiparameter was afterward overlapped to build a vulnerability map while also considering the geological dataset and validated by ground verification. This finding will be presented to the section of the city that can help support its future growth in terms of its vulnerability to dangers caused by land subsidence.

Keywords: Geographic Information System, Land Subsidence, Remote Sensing, Semarang City, Vulnerability Assessment

Abstrak. *Penurunan tanah merupakan isu yang signifikan pada masa kini, terutama di beberapa wilayah di mana hal ini memiliki potensi untuk mengganggu perkembangan masa depan, menghentikan proses, dan bahkan mengubah rencana pembangunan. Penelitian ini secara umum berfokus pada pembaruan pengetahuan terkini mengenai penurunan tanah dan melakukan penilaian risiko menggunakan studi kasus di Kota Semarang, Jawa Tengah, di mana penurunan tanah merupakan masalah serius. Beberapa citra satelit, seperti Sentinel-1 dan Sentinel-2, digunakan sebagai basis data dalam penelitian ini, dengan berbagai analisis target dan metode Sistem Informasi Geografis (SIG) digunakan untuk mengelola dan memodifikasi data. Data radar Sentinel-1, bersama pendekatan analisis pergeseran* Differential Interferometry Synthetic Aperture Radar *(DInSAR), utamanya digunakan untuk memberikan gambaran keadaan saat ini dari penurunan tanah di daerah ini pada tahun 2022. Hasilnya menunjukkan variasi nilai pergeseran vertikal berkisar antara -7,7 hingga 6,65 cm dengan penurunan tanah terutama menyebar di wilayah utara, menggunakan dua set data dengan selang waktu 60 hari antara Januari dan Maret. Menggunakan kombinasi* Normalize Difference Vegetation Index *(NDVI) dan* Normalize Difference Built-in Index *(NDBI) untuk membuat data* Built-up Index *(BU), data Sentinel-2 dengan citra berbasis optik kemudian digunakan untuk memetakan fitur buatan manusia dan perluasan, terutama bangunan. Setiap informasi yang dianggap multiparameter kemudian tumpang tindih untuk membangun peta kerentanan bersamaan dengan juga mempertimbangkan dataset geologis dan divalidasi melalui verifikasi lapangan. Temuan ini akan disampaikan kepada bagian kota yang dapat membantu mendukung pertumbuhannya di masa depan dalam hal kerentanannya terhadap bahaya yang disebabkan oleh penurunan tanah.*

Kata Kunci: *Sistem Informasi Geografis, penurunan tanah, penginderaan jauh, Kota Semarang, penilaian kerentanan*

1. Introduction

Semarang City is one of the largest cities on Java Island's coast (see Figure 1), and it has been threatened with deterioration in the past, present, and future owing to land subsidence. The significant extraction of groundwater, which began to be intensive to excessive in the early 1980s and was directly proportional to the number of groundwater extraction wells (Marfai and King, 2007), influenced the decline in land values in this area in the lowest value range of 0 to more than 15 cm/year (Abidin et al., 2013). Excessive fluid extraction causes compaction of coastal sediment deposits in the form of alluvial deposits, which accommodate pore-filling fluid, producing grain redistribution vertically and laterally (Sarah et al., 2020). If it persists or worsens, this condition might threaten Semarang City's future growth, necessitating quick effort to determine whether parts of the city are more vulnerable to land subsidence than others.

Land subsidence has been measured and monitored in Semarang City for an extended period using various methods. The first study began in 1983 and is still ongoing (Marfai and King, 2007; Marfai and King, 2008). Land subsidence is detected in Semarang City using a variety of approaches, ranging from in-situ assessments utilizing Global Positioning Systems (GPS) data to remote sensing data (Abidin et al., 2013; Abidin et al., 2010; Bott et al., 2021; Kuehn et al., 2010). However, in the study region, information on the present state of land subsidence (in 2022) and land subsidence vulnerability assessment has not been evaluated or made accessible in a new publication.

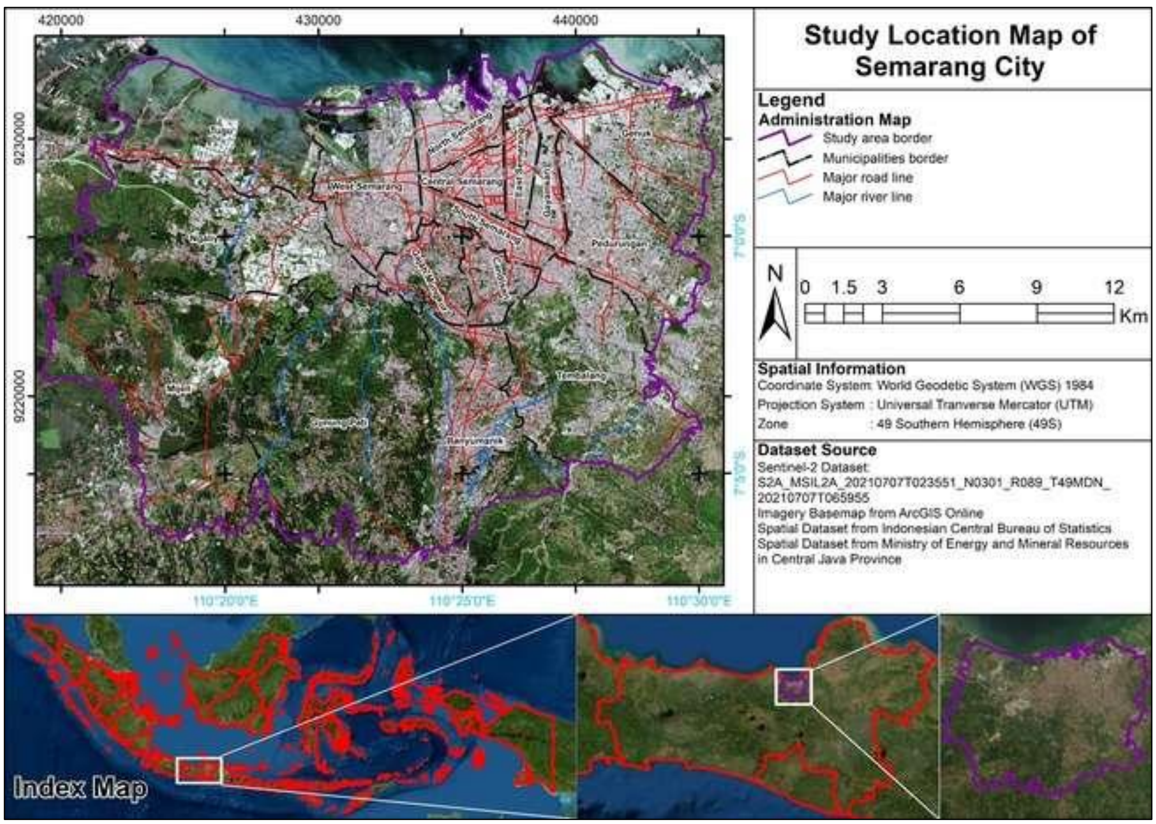

Figure 1 Map showing the study location in Semarang City.

2. Data and Method

Several datasets, including satellite imagery, geographic data, and field approach data, are utilized to support each outcome in this study. Each dataset is an example application for the findings to be provided in relation to recognizing the current land subsidence aspect in Semarang and indicating the outcome of a land subsidence vulnerability assessment.

The initial dataset, satellite imaging data, was provided by the European Space Agency (ESA) as part of the Sentinel project within the https://search.asf.alaska.edu/ and https://scihub.copernicus.eu/ website. Both sources offer two types of satellite images: Sentinel-1 radar-based imaging data and Sentinel-2 optical-based imagery data. The Sentinel-1 collection comprises C-band data with a resolution of 5x20 m and a data interval of 6 to 12 days on each acquisition. These were utilized to recover elevation feature change in two similar datasets at different dates using phase information. The DInSAR approach is utilized to generate the needed data with a particular methodology for extracting the subsidence value (Braun, 2021) in the present time or 2022. Sentinel-2, on the other hand, is the second dataset and consists primarily of sensor-extracted optical features for a variety of applications, including land use, climate change, and catastrophe assessment, with high-resolution data (Phiri et al., 2019). This type of data is utilized in this study to determine the distribution of vegetation and manmade objects, particularly dwellings (Zha et al., 2003; He et al., 2010), using the Normalize Difference Vegetation Index (NDVI), the Normalize Difference Built-up Index (NDBI), and the Built-up Index (BU). Equation 1 to equation 3 are utilized to remove data from the Sentinel-2 collection to create that information. See Table 1 for further information on the imaging data utilized.

$$\text{NDVI} = \frac{(\text{NIR Band - Red Band})}{(\text{NIR Band + Red Band})} \tag{1}$$

$$\text{NDBI} = \frac{(\text{SWIR Band - NIR Band})}{(\text{SWIR Band + NIR Band})} \tag{2}$$

$$\text{BU} = \text{NDBI - NDVI} \tag{3}$$

Table 1 List of Satellite Imagery used in the current study

Satellite Imagery Datasets	Resolution	Name of Each Metadata
Sentinel-1 (Radar-based)	10 m	S1A_IW_SLC__1SDV_20220101T221729_20220101T221756_041273_04E7D1_EA01 and S1A_IW_SLC__1SDV_20220302T221727_20220302T221754_ 042148_0505A9_AEBF
Sentinel-2 (Optical-based)	10 m	S2A_MSIL2A_20210707T023551_N0301_R089_T49MDN_20210707T065955

Geospatial data, the third dataset, may be integrated and stand-alone to complement this study using satellite imaging data. The data was utilized to study Semarang's regional geology and hydrogeology, which was later validated by a field method. The field approach dataset also indicates the outcome of land subsidence in Semarang and proves the lithological variance in the study region.

Land subsidence vulnerability (LSV) maps are then analyzed based on the previous data to determine the susceptibility in this topic by overlaying each parameter into one primary map. Apart from the Subsidence value (S), three other spatial datasets are examined in this study to be utilized as natural and artificial representations for building the final map: Geology (G), Hydrogeology (H), and Built-in area (B). In Equation 4, all parameters are computed with the same weight in a 100 percent value (25 percent for each parameter) and then added together. This equation was created by the author in response to no specific study about land subsidence vulnerability assessment, particularly in Semarang City. Later, the high-vulnerability areas are surveyed directly in the field to determine the presence of land subsidence and the impact or outcome on any objects present. This vulnerability assessment's final score will be a discrete number ranging from low vulnerability to small value and vice versa.

$$\text{LSV} = (G*0.25)+(H*0.25)+(B*0.25)+(S*0.25) \tag{4}$$

3. Result and Discussion

3.1 Overview of Natural and Artificial Parameter Distribution

The initiating or exacerbating component of land subsidence in a given location is often due to geological, hydrogeological, and human activity. To summarize, the kind of rock formation that causes land subsidence, the hydrogeological region where

people take groundwater and damage the aquifer, and the presence of an artificial structure on the surface that raises the overburden are all factors to consider.
The study region is divided into four lithological units: surficial deposits (SD), volcanic rocks (VR), intrusive rocks (IR), and sedimentary rocks (SR), as shown in the geological map of Magelang and Semarang (Thanden et al., 1996) (Figure 2A). The distribution of each type is highly segregated, starting with the unconsolidated combination of gravel, sand, and clay in the north and progressively shifting south to volcanic and intrusive rocks. The central portion of the study area is exceptional because it contains older sedimentary rock that has been elevated and exposed on the surface. Several outcrops are found through the field survey represented in the list above; see Figure 3A to 3D.

The hydrogeological aspect (Figure 2B) is based on the amount and occurrence capability of subterranean groundwater aquifers. In this regard, the study area is separated into four regions: productive aquifers with moderate dispersion, moderate productive aquifers, localized groundwater aquifers, and rare groundwater occurrence regions (Said and Sukrisno, 1988). The first category includes groundwater occurrence regions that exist and flow in intergranular, with total yields of less than 5 liters per second. Aquifers that flow through fissures, cracks, and channels with variations in groundwater discharge are included in the second and third categories. The fourth class includes areas where there is no highly accessible groundwater or where groundwater is found far below the usual depth.

In order to distinguish between artificial landcover and natural land cover (vegetation), a false-color composite based on Sentinel-2 data that indicates the high reflectance of such an item (in this example, Band 12, 11, and 4) is utilized (or 7-6-4 in Landsat-8). Artificial infrastructure and barren areas/open fields are depicted in bright colors, whereas flora is shown in green, and water bodies are described in blue (Figure 2C) and discussed further in the following part.

To confirm this result, the BU result indicating the lateral distribution of the constructed area in Semarang City is compiled from the computation between the NDVI and NDBI, as described in the preceding equation (Figures 2D and 2E). In Semarang, the NDVI represents the distribution of vegetation. The NDBI result, on the other hand, displays a lower value for vegetation (0) and a more considerable value for artificial features (open spaces or structures), both of which have a value greater than 0. The final distribution and separation between artificial features and vegetation area was determined using the NDBI and NDVI, with a limitation value higher than -0.75 for built-area or artificial features and lower than that value for non-artificial features, especially vegetated areas (forest, rice field, and bushes). The BU value result (Figure 2F), which ranged from -1.562 to 1.989, later confirmed that the built area is primarily distributed in the northern part of Semarang City, with extensions to the east, central, and southeast regions, and several fully vegetated areas to the west and southwest and partially isolated across the area.

3.2 *Current Land Subsidence Value*

The DInSAR technique determines displacement values for two acquisitions from January 1st to March 2nd, 2022. According to this finding, the maximum subsidence value is slightly lower, about -0.067 m or -6.7 cm, whereas the highest uplift value is around 0.077 m or 7.7 cm (Figure 4). According to the map, the areas that experience evident sinking in 2022 are

Spread in the northwest (Tugu), northeast (Genuk and Pedurungan), and partially in the southwest (Ngaliyan and Mijen). On the other hand, a considerably raised region may be found in the study area's south-eastern corner (Tembalang and Banyumanik). For the rest of the study area, where there is no smooth or distinct distribution, subsidence and uplift are contained simultaneously in one place, such as at Mijen, Gunungpati, and Candisari.

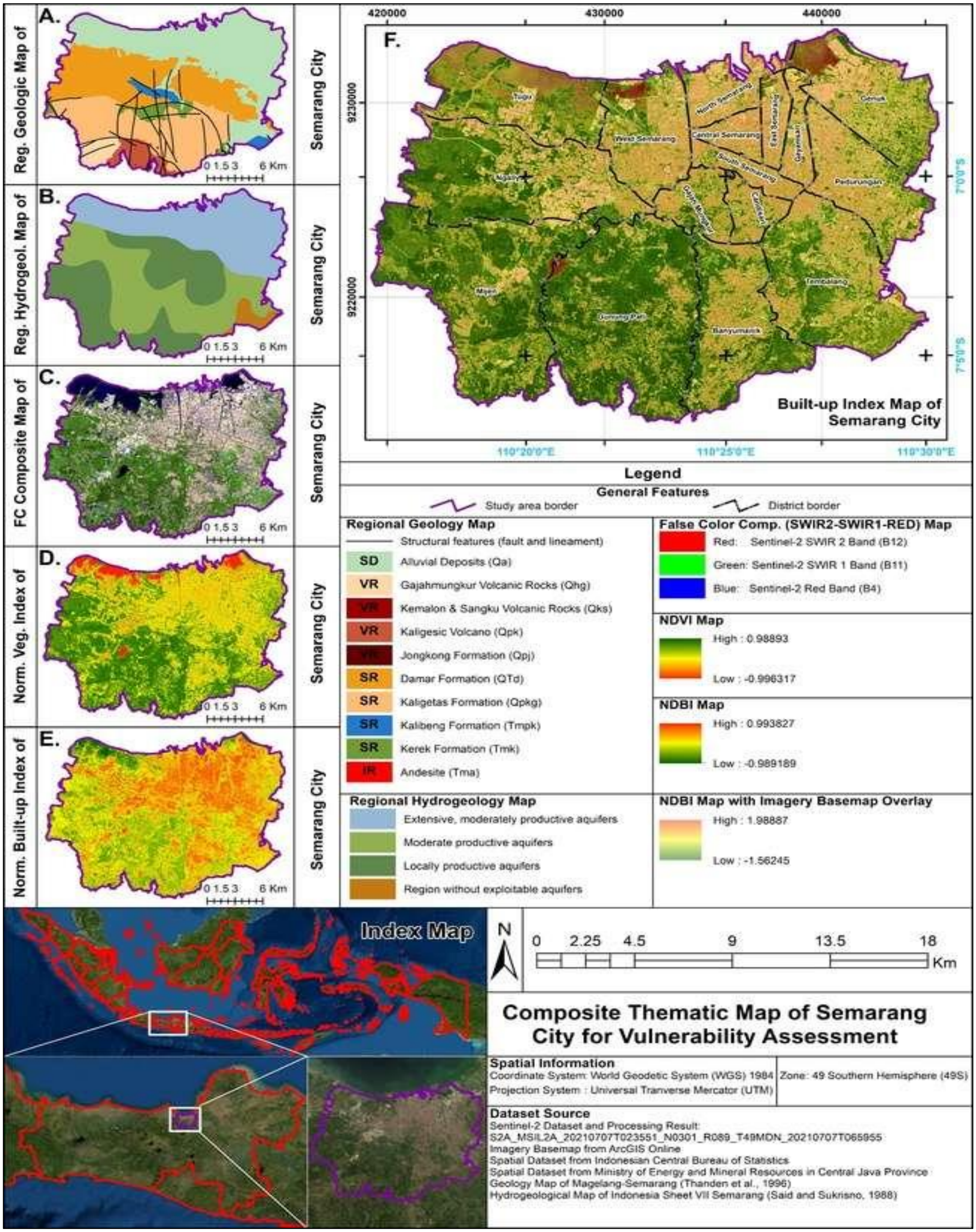

Figure 2 Several thematic maps illustrating various aspects of the study: (A) regional geological map as baseline for G parameter, (B) hydrogeological map as baseline for H parameter, (C) false colour composite using Sentinel-2 for distinguishing artificial and natural features, (D) NDVI calculation result, (E) NDBI calculation result, and (F) BU calculation result based on NDVI and NDBI as B parameter.

Figure 3 Several photographs from a field survey conducted to confirm and support the regional geology maps, with several key formations as representative: Kerek Formation (A), Kaligetas Formation (B), Damar Formation (C), and Alluvium (D).

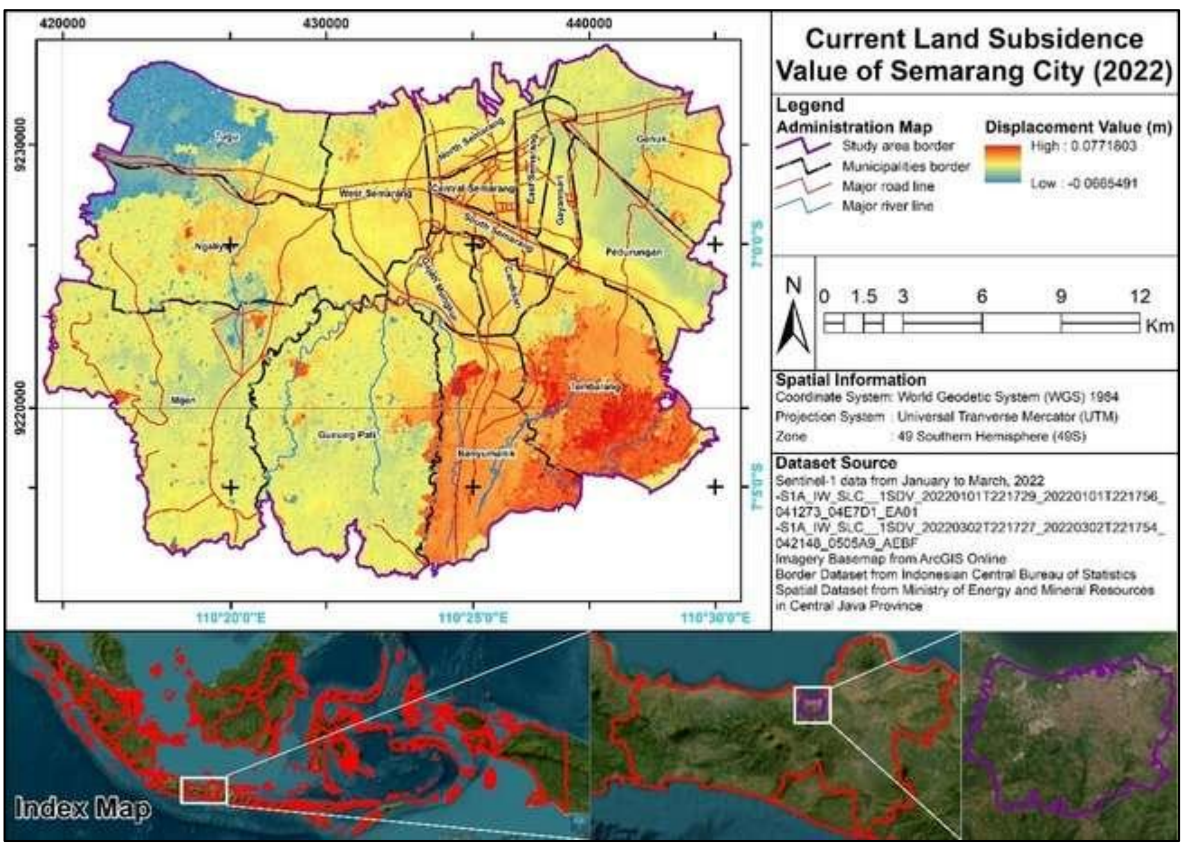

Figure 4 Result of the current land subsidence value using the DInSAR method in 2022 as the baseline for the S parameter.

3.3 Vulnerability Assessment and Field Survey Comparison

For further analysis, all parameters must be distinguished depending on the magnitude of the influence on the phenomena while analyzing the susceptibility of land subsidence in the study region, as explained in Equation 4 above. Low- and high-class kinds are assigned to three parameters (geology, hydrogeology, and built-in index). Each class is assigned a numerical number, with one indicating low and two signifying high.

Separate classifications are developed for each parameter based on the distribution of land subsidence observed in the current and previous studies. According to the DInSAR displacement results, land subsidence occurred mostly on alluvium sediment for the geology portion, on a reasonably productive aquifer where land subsidence may be attributed to groundwater abstraction, and in densely inhabited areas. All of these variables are accounted for in the high value (with a value equal to two). Apart from the allocated high-value class, the other class will represent low-value and have an equal value. As shown in Figures 5A to 5E, the current land subsidence parameter is further divided into two classes: subside area (represented by a negative number with a value of two (high) and non-subside area (shown by positive remarks with a value of one (low).

Regarding the distribution area, the land subsidence vulnerabilities depicted in the previous images exhibit significant parallels and variances. As a consequence of the equation utilized, the high vulnerability region has a value near two, while the low vulnerability area has a value close to one.

The northern half of the study region has a high sensitivity score for direct land subsidence, with expansions to the northeast and northwest and partially to the southeast and southwest. Based on this, the northern section of Semarang City and a few other areas distributed across the city are characterized as generally highly exposed to land subsidence hazards, with a value close to 2. Numerous field visits with high vulnerability values were done, yielding 19 points that reflect the land subsidence-affected feature. The influence or impact on infrastructure and structures, such as dwellings, roads, bridges, and utility poles (Figures 5F to 5I).

3.4 Implementation of Vulnerability Map and Future Study Needs

The land subsidence vulnerability map includes several factors and is also being examined for use in the study area's future development. Due to many negative aspects like geology, hydrogeology, land subsidence phenomena, and artificial elements, the northern part of Semarang City is not desirable for future development when assessing the ultimate appropriateness conclusion.

To be more precise, numerous studies have demonstrated that the long-term growth of unstable alluvial deposits might offer a long-term concern. If there are multiple clay and sand deposits in recent alluvial deposits, they will tend to compress over time until stabilization (Sarah et al., 2020; Lo et al., 2021). In the same vein, the hydrogeological aspect interacted with the geological element at the same time. Many people extract water from alluvial deposits, well-known fresh groundwater supplies worldwide (Dimkić et al., 2011; Mukherjee, 2018). The abstraction rate is high in the study region and rises dramatically with each newly dug well, whether registered or unregistered (Abidin et al., 2013). In specific ways, groundwater aquifers compensate for fluid loss, and deformation that may cause compaction, such as the effective stress, is reversible (Ojha et al., 2019; Smith et al., 2017). The aquifer's deformation will be irreversible and permanent if the limit is exceeded.

According to the vulnerability result, avoiding some sections and focusing on other portions is strongly urged to be adopted to keep future development on track. While ground subsidence poses a long-term hazard to infrastructure development, further precautions should be taken for Semarang City's coastline area. A greater emphasis should be placed on the southern half, which is more stable regarding geology, hydrology, and land subsidence. Regions with a low vulnerability value can be further developed more effectively.

BULLETIN OF GEOLOGY, VOL. 7, NO. 4, 2023
DOI: 10.5614/bull.geol.2023.7.4.1

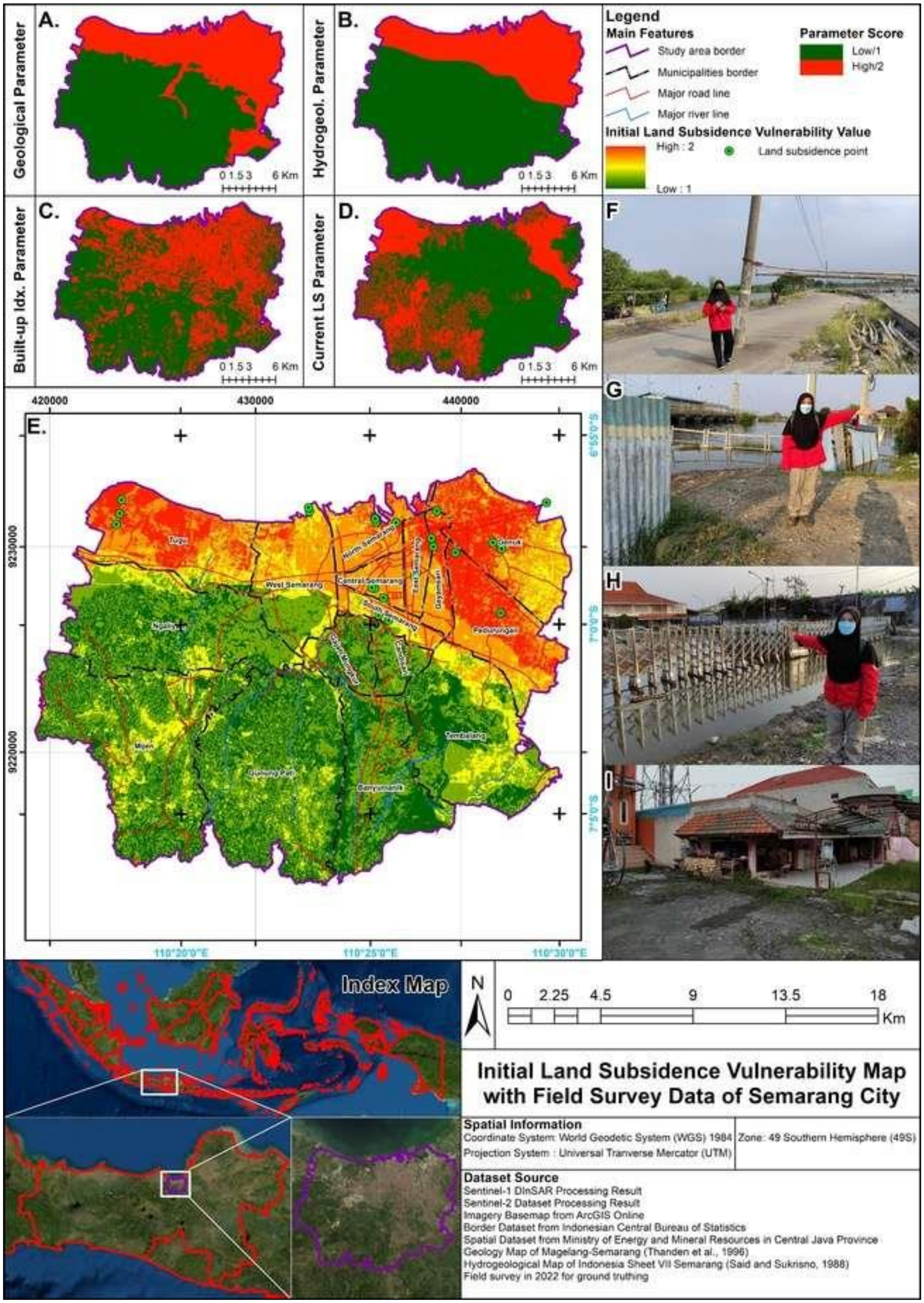

Figure 5 Several maps depicting classified information for each vulnerability assessment parameter, including G parameter (A), H parameter (B), B parameter (C), S parameter (D), and vulnerability calculation result (E) indicating low to high vulnerability region. Those datasets are accompanied by many photographs taken during a field study in a high-vulnerability region, showing the objects touched by land subsidence, such as tilting utility poles (F), drowned or subsided infrastructure, and ground-altered buildings (G to I).

Because the contained parameters are insufficient, the final land subsidence vulnerability maps created from this study are not deemed final. As an initial remark, with all of the data availability issues and sufficient parameters used, this study should hopefully prompt a more comprehensive study to assess land subsidence hazard in greater detail, which should be highly recommended to policymakers and stakeholders as an initial consideration for future development programs.

4. Conclusion

The vulnerability assessment in this study considered several factors that influence land subsidence in the worst-case scenario, including geology, hydrogeology, and the artificial component of humanity derived from spatial datasets and optical remote sensing data. Two pairs of radar-based datasets were utilized to construct land subsidence values in 2022 as the significant comparison, from January to March (direct processing), with values ranging from -6.7 cm as the least and 8.1 cm as the most significant displacement. A separate class for each parameter with a difference generally with the link to land subsidence was created from the parameter for vulnerability assessment: strongly impacting (value two) and weakly affecting (value one) (value one). Land subsidence is mainly distributed on alluvium deposits with a high occurrence of groundwater aquifers and high-density regions with diverse structures compared to other criteria. The vulnerability map constructed using the listed equation and equal weighting with a final value of one to two shows that the northern area is vulnerable to land subsidence, with extensions to the east, west, and partially southeast. While more study is needed to corroborate the vulnerability strategy utilized, this conclusion can be used by the government or local stakeholders as a factor for future development planning.

Acknowledgments

The authors thank N. Santi, particularly, and the members of the Geological Engineering Department of Diponegoro University, which supports the field data acquisition. S. Aghnia's colleagues supplied the necessary data for the geospatial analysis within this study. This research was supported by the author's self-funding with regard to his colleagues.

REFERENCES

Abidin H. Z., Andreas H., Gumilar I., Sidiq T. P., Fukuda Y. (2013). Land subsidence in coastal city of Semarang (Indonesia): Characteristics, impacts and causes. *Geomatics, Natural Hazards and Risk* 4(3):226–40.

Abidin H. Z., Andreas H., Gumilar I., Sidiq T. P., Gamal M., Murdohardono D. (2010) Studying Land Subsidence in Semarang (Indonesia) using Geodetic Methods. *FIG Congress* (April 2010):11–6.

Bott L.M., Schöne T., Illigner J., Haghshenas Haghighi M., Gisevius K., Braun B. (2021). Land subsidence in Jakarta and Semarang Bay – The relationship between physical processes, risk perception, and household adaptation. *Ocean Coast Manag.* 211.

Braun A. (2021) Retrieval of digital elevation models from Sentinel-1 radar data - Open applications, techniques, and limitations. *Open Geosciences* 13(1):532–69.

Dimkić M., Pušić M., Majkić-dursun B., Obradović V. (2011). Certain Implications of Oxic Conditions in Alluvial Groundwater. *Water Research and Management* 1(2):27–43.

He C., Shi P., Xie D., Zhao Y. (2010). Improving the normalized difference built-up index to map urban built-up areas using a semiautomatic segmentation approach. *Remote Sensing Letters* 1(4):213–21.

Kuehn F., Albiol D., Cooksley G., Duro J., Granda J., Haas S. (2010). Detection of land subsidence in Semarang, Indonesia, using stable points network (SPN) technique. *Environ Earth Sci.* 60(5):909–21.

Lo W., Purnomo S.N., Sarah D., Aghnia S., Hardini P. (2021). Groundwater modelling in urban development to achieve sustainability of groundwater resources: A case study of Semarang city, Indonesia. *Water* (Switzerland)13(10).

Marfai M.A., King L. (2007).Monitoring land subsidence in Semarang, Indonesia. *Environmental Geology* 53(3):651–9.

Marfai M.A., King L. (2008). Tidal inundation mapping under enhanced land subsidence in

Semarang, Central Java Indonesia. *Natural Hazards*. 44(1):93–109.

Mukherjee A. (2018). Overview of the Groundwater of South Asia. In: Mukherjee A, editor. Groundwater of South Asia [Internet]. Springer Nature Singapore Pte Ltd.; p. 3–20. Available from: http://link.springer.com/10.1007/978-981-10-3889-1_1

Ojha C., Werth S., Shirzaei M. (2019). Groundwater Loss and Aquifer System Compaction in San Joaquin Valley During 2012–2015 Drought. *J Geophys Res Solid Earth* 124(3):3127–43.

Phiri D., Simwanda M., Salekin S., Ryirenda V.R., Murayama Y., Ranagalage M., (2019). Remote sensing Sentinel-2 Data for Land Cover / Use Mapping: A Review. *Remote Sensing* 42(3):14.

Said H.D., Sukrisno. (1988). *Hydrogeological map of Indonesia: Sheet VII Semarang (Java)* scale, 1:250.000.

Sarah D., Hutasoit L.M., Delinom R.M., Sadisun I.A. (2020). Natural Compaction of Semarang-Demak Alluvial Plain and Its Relationship to the Present Land Subsidence. *Indonesian Journal on Geoscience* 7(3):273–89.

Smith R.G., Knight R., Chen J., Reeves J.A., Zebker H.A., Farr T.(2017). Estimating the permanent loss of groundwater storage in the southern San Joaquin Valley, California. *Water Resour Res* 53(3):2133–48. http://doi.wiley.com/10.1002/2016WR019861

Thanden R.E., Sumadirdja H., Richards P.W., Sutisna K., Amin T.C. (1996). *Geological Map of the Magelang and Semarang Sheets, Jawa*, scale 1: 100: 000. Geological Research and Development Centre, Bandung.

Zha Y., Gao J., Ni S. (2003). Use of normalized difference built-up index in automatically mapping urban areas from TM imagery. *International Journal of Remote Sensing* 24(3):583–94.